

promoting access to White Rose research papers



Universities of Leeds, Sheffield and York
<http://eprints.whiterose.ac.uk/>

This is an author produced version of a paper published in **Tribology Transactions**.

White Rose Research Online URL for this paper:
<http://eprints.whiterose.ac.uk/9164/>

Published paper

Reddyhoff, T., Dwyer-Joyce, R.S. and Harper, P. A new approach for the measurement of film thickness in liquid face seals. *Tribology Transactions*, 2008, **51**(2), 140-149.

[http://dx.doi.org/ 10.1080/10402000801918080](http://dx.doi.org/10.1080/10402000801918080)

A New Approach for the Measurement of Film Thickness in Liquid Face Seals

T. Reddyhoff, R.S. Dwyer-Joyce, P. Harper.

Department of Mechanical Engineering,
Mappin Street, University of Sheffield, Sheffield S1 3JD, UK

Abstract

Face seals operate by allowing a small volume of the sealed fluid to escape and form a thin film between the contacting parts. The thickness of this film must be optimised to ensure the faces are separated, yet the leakage is minimised. In this work the liquid film is measured using a novel ultrasonic approach with a view to developing a condition monitoring tool.

The trials were performed in two stages. Initially tests were based on a lab simulation, where it was possible to compare ultrasonic film thickness measurements with optical interference methods and capacitance methods. A direct correlation was seen between ultrasonic measurements and capacitance. Where ultrasonic and optical methods overlap, good correlation is observed, however the optical method will not record film thickness above $\sim 0.72\mu\text{m}$.

A second set of trials was carried out, where the film thickness was monitored inside a seal test apparatus. Film thickness was successfully recorded as speed and load was varied. The results showed that while stationary the film thickness varied noticeably with load. When rotating however, the oil film remained relatively stable around $2\mu\text{m}$. During normal operation of the seal, both sudden speed and load changes were applied in order to initiate a seal failure. During these events, the measured film thickness was seen to drop dramatically down to $0.2\mu\text{m}$. This demonstrated the ability of the technique to predict failure in a face seal and therefore its aptitude for condition monitoring.

1. Introduction

In many rotating fluid machinery applications (pumps, turbines, compressors etc) a rotating shaft enters a chamber containing a pressurized fluid. Mechanical face seals are used to seal the chamber whilst allowing shaft rotation. Their operation relies on a thin film of fluid to separate rotating and a stationary seal faces. The thickness of the fluid film is of critical importance, it must be sufficiently thick that friction (torque) and wear are low, but not so thick that excessive leakage occurs. The flow rate through the seal is typically proportional to the cube of the seal face separation [1]. Increasing environmental restrictions on fluid leakage make this a significant issue.

Seal failure occurs as a result of contact between seal faces, after the fluid film has broken down. To avoid catastrophic failure seals must be routinely maintained. Much attention has been given to condition monitoring of seals, in order to reduce maintenance schedules and the potential for costly failures.

Many authors have carried out work based on acoustic emission; this involves mounting an acoustic sensor on a seal and using it to listen for the sound waves generated as a result of contacting seal faces. A good example of this is work carried out by Miettinen et al [2] where acoustic emission sensors were used monitored on a face seal in a centrifugal pump. The shortfall of these techniques is that presence of background noise (unavoidable in

industrial applications) makes the acoustic emission from contacting seal faces difficult to isolate.

A more robust technique is that which uses an active ultrasonic shear sensor as developed by Anderson et al [3]. Ultrasonic sensors are mounted on a seal face such that the shear wave reflection from the seal interface can be monitored. Shear wave propagation through a liquid is negligible therefore the shear wave reflection is only reduced by the existence of contacting seal faces. In this way seal face contact can be detected. The disadvantage of this technique is that it only detects when contact has already occurred, and cannot be used to measure film thickness during normal separation.

Electrical resistance and capacitance have proved useful methods in general film thickness measurement, as have optical methods. However, both these approaches require modifications (electrical contacts and an optical window, respectively) to the bearing machinery that hinder their practical application to seal monitoring [4-8].

A promising technique for the monitoring of fluid film thickness is that using the reflection of longitudinal ultrasonic waves [9]. In common with shear reflection, this can be used on original bearing parts and does not require any contact with the liquid film. An incident ultrasonic pulse will be partially reflected from an oil film. The proportion reflected can be related to the thickness of the oil film using a quasi-static spring model (provided the acoustic properties of the bearing materials and the oil are known).

The method has been developed on laboratory oil films in elastohydrodynamic [10] and hydrodynamic [11] contacts. In principle the method can be used for a wide range of liquid layers trapped between solid surfaces. However the acoustic and attenuative properties of the three-layer system require certain frequencies to be used. Not all measurements are therefore feasible or indeed practical.

This paper describes a series of trials carried out to measure the fluid film formed by a face seal against a rotating flat followed by a set of tests carried out on a seal test rig.

2. Background

If ultrasound is incident on a layered system then some of the wave will be reflected at the front face of the layer and some at the back face. For thin layers, the reflected pulses overlap and it becomes impossible to distinguish the discrete reflections in the time domain. If the lubricant film thickness is very thin then the layer behaves like a spring and the reflection of the wave depends on the spring stiffness.

By considering the equilibrium of forces and compatibility at the boundaries of the layer during the passage of the wave, it is possible to show the dependence of the reflection on interface stiffness [12]. In this way, Tattersall [13] demonstrated that the reflection coefficient of a thin layer between two media was given by the expression:

$$R = \frac{z_1 - z_2 + i\omega(z_1 z_2 / K)}{z_1 + z_2 + i\omega(z_1 z_2 / K)} \quad (1)$$

Where z_1 and z_2 are the acoustic impedance of the media either side of the layer, ω is the angular frequency ($\omega = 2\pi f$) and K is the interfacial stiffness. An important observation from the above relation shows the dependency of the reflection coefficient on interfacial stiffness. If a liquid film is present between the two surfaces, then the layer stiffness (the rate of change of pressure with approach of the surfaces) is related to the thickness of film h simply by:

$$K = \frac{B}{h} \quad (2)$$

where B is the bulk modulus of the oil film. It should be noted, at this stage, that this assumes that the surfaces are perfectly smooth and parallel.

Combining (1) and (2) and rearranging gives the film thickness in terms of the reflection coefficient amplitude $|R|$.

$$h = \frac{\rho c^2}{\omega z_1 z_2} \sqrt{\frac{|R|^2 (z_1 + z_2)^2 - (z_1 - z_2)^2}{1 - |R|^2}} \quad (3)$$

Inspection of equation (3) shows that, as expected, higher frequencies allow thinner films to be measured. The value of the reflection coefficient varies from $(z_1 - z_2)/(z_1 + z_2)$ to 1 as the film varies from zero to infinity. But typically the best measurements are achieved for $1.05 \times (z_1 - z_2)/(z_1 + z_2) < R < 0.95$ as the effect of noise in the recorded signal is significant outside this range.

The range of measurable film thickness can then be calculated for a given frequency and material combination (z_1 and z_2). Table 1 shows the result (all values are approximate and depend on the signal to noise ratio) for different material combination cases and sample acoustic frequencies.

Material	Measurable film thickness range μm		
	f=6MHz	f=15MHz	f=25MHz
Silicon carbide-glass	0.23-9.11	0.09-3.64	0.06-2.19
Silicon carbide-steel	0.14-5.79	0.06-2.32	0.03-1.39
Silicon carbide-silicon	0.1-7.24	0.05-2.90	0.03-1.74

Table 1. Approximate minimum measurable film thickness for different combinations of seal material pairs with three measuring frequencies.

3. Evaluation Experiments

3.1 Apparatus

A silicon carbide test seal was pressed against a disk counterface using on a modified WAM5 rig (from Wedevan Associates Inc.), as shown in Figure 1. Controls on the rig allowed the disc to be rotated at varying speed and load relative to the ring, whilst allowing film thickness to be measured optically (using a glass disk) or with a capacitance technique (using a steel disk). Figure 1 schematically shows the configuration.

A piezoelectric element was glued to the bottom face of the silicon carbide ring. The element was driven by an ultrasonic pulser receiver (UPR), which in turn was connected to a digital oscilloscope and PC. The UPR generated a controlled top hat voltage pulse, which excited the piezoelectric element in the transducer causing it to resonate, thus sending the required ultrasonic pulse through the medium. The piezoelectric element then received reflected waves, emitted voltage pulses, which were then stored on the digital oscilloscope, before being passed on to the PC for appropriate signal processing. The PC controlled the UPR,

performed the signal processing, and displayed results with software written in the Labview environment.

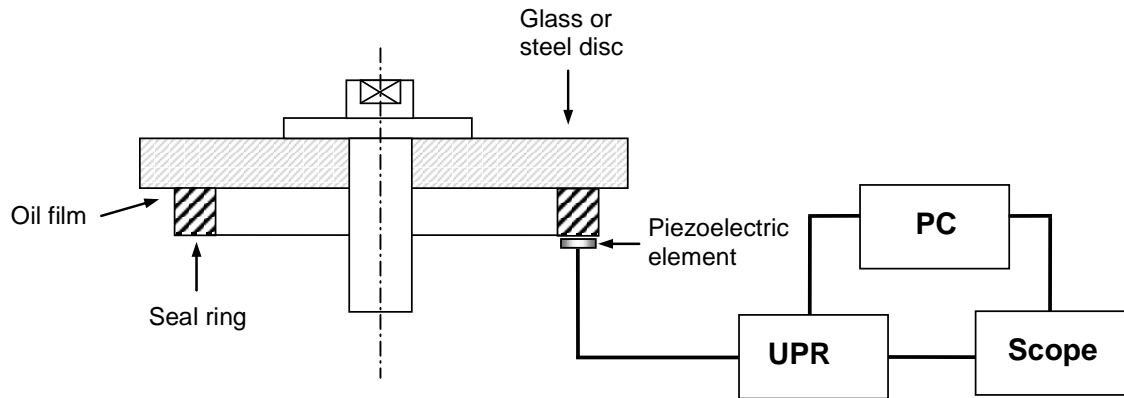


Figure 1. Schematic diagram of the equipment showing the glass or steel disk, silicon carbide seal and the ultrasonic apparatus.

Ultrasonic Transducers

The piezoelectric elements used, operated in pulse-echo mode so they could send and receive pulses to and from the liquid film. The piezoelectric elements were constructed from Lead Zirconate Titanate (PZT), with a nominal centre frequency of 10MHz. A wrap around electrode construction was required as SiC is an electrical insulator. Piezoelectric elements were chosen over conventional manufactured ultrasonic transducers due to their reduced size and cost. The elements were bonded directly onto the seal back (i.e. non-contacting) face and wires soldered directly to the electrodes.

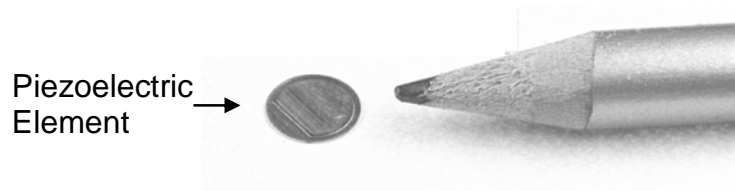


Figure 2. Photograph showing relative sizes of ultrasonic transducer and piezoelectric element.

Acoustic Material Properties

It is important that exact values of acoustic impedance are found, as errors as low as 5% can have a significant effect on the calculated film thickness especially at low reflection coefficient values.

Both the glass and steel disks and the SiC ring have a simple geometry, and so the volume of the components can be calculated with a reasonable degree of accuracy. The mass of each of the components was measured with an electronic balance, while the associated speed of sound was found ultrasonically. The acoustic impedances of the ring and disk were therefore calculated accurately using the equation (4).

$$z = \rho c \quad (4)$$

The material properties found in this way for the four materials used (silicon carbide, glass, steel, and T32 mineral oil) are shown below in Table 2.

	Density,	Speed of sound, <i>c</i> , m/s	Acoustic impedance,

	$\rho, \text{kg/m}^3$		$z, \text{kg/m}^2\text{s} \times 10^6$
Silicon Carbide	2690	10835	29.2
Glass	2850	5728	16.3
Oil T32 (at room temp)	859	1235	1.06
Steel	7760	5880	45.6

Table 2. Acoustic Properties of Materials Used in the Study.

Ultrasonic Measurement of Oil Films

Once the rig was assembled, a reflection was taken from the glass/air interface (that is equivalent to the incident signal). This signal was then passed through a Fourier transform in order to give the incident reference spectrum. The transducer was then located at a point in line with the oil/glass interface. Subsequent reflections were taken and Fourier transformed and divided by the reference to give a reflection coefficient amplitude spectrum. Equation (3) was then employed to calculate the film thickness. The measured film thickness was displayed in real time on the PC (reflection coefficient spectra, pulse amplitudes, and film thickness data are stored for post-processing). This method is described in more detail in references [9,10].

Optical Interference Method

The film thickness between faces of the seal was also measured optically using the WAM5 machine. The principle on which the WAM rig operates was first developed by Cameron et al [7] and relies on interference of light waves to establish film thickness. The system was automated so that the fringe pattern is directly converted to an oil film thickness. In practice measurements of film thickness greater than $0.72 \mu\text{m}$ were not possible, as this represents the coherence limit for light.

Capacitance Method

The Lubcheck equipment (developed by SKF), based on capacitance measurement was also used for comparisons. For this, the glass disc on the WAM5 rig was replaced by a steel disk. The capacitance between the seal and plate was continually recorded. The capacitance C is inversely proportional to the distance y between faces.

$$C = \varepsilon_0 \varepsilon_r \left(\frac{A}{y} \right) \quad (7)$$

where A is a constant and ε_0 and ε_r are the permittivity of free space and of the oil gap respectively. Details of this technique are given in reference [14]. Whilst C is inversely proportional to the gap between the plates, it is not possible to give a unique film thickness without some alternative calibration to determine the capacitance of an oil layer. In this work an independent calibration was not performed and linearity only was studied.

3.2. Results

Simultaneous Measurement using Optical Interference and Ultrasonic Methods

The aim of first set of trials was to compare the optical and ultrasonic film thickness measurements. The glass disc, which was known to have significant surface waviness, was

rotated at a low speed. Figure 3 shows the optical and ultrasonic plots of the thickness of gap between the seal faces.

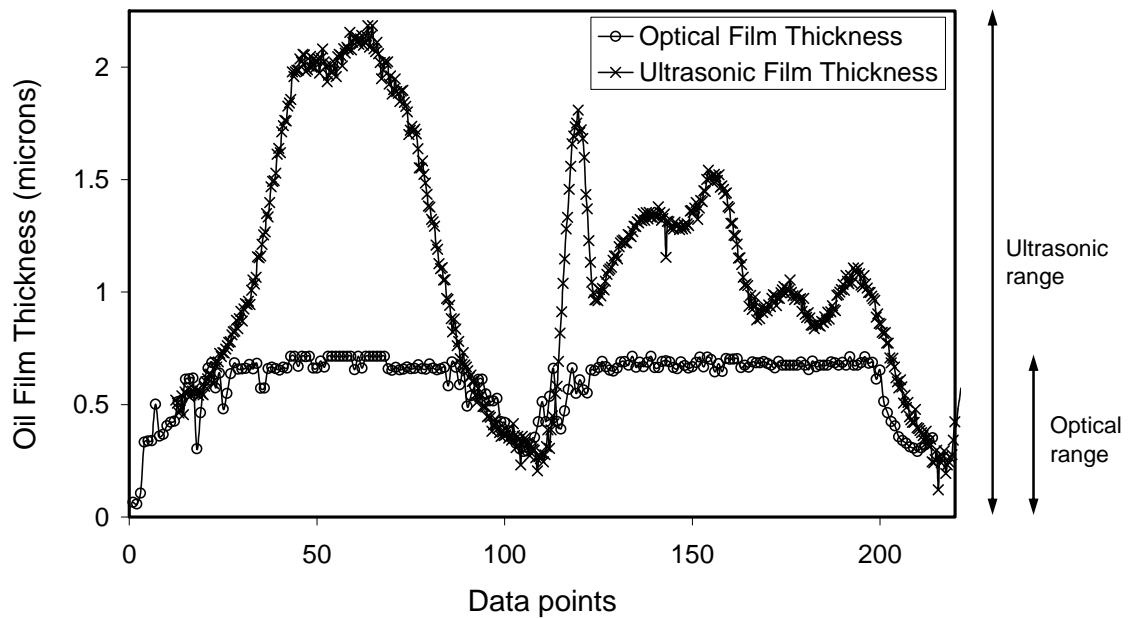


Figure 3. Comparison of ultrasonic and optical measured film thickness as the glass disc is rotated.

The maximum measurable film by the optical technique is $\sim 0.72\mu\text{m}$. So the method tops out at this value. Where the optical limit is exceeded (data points 25-80 and 125-200) the ultrasonic method continues reading. In the regions where both techniques are operating, there is good agreement between ultrasonic and optical measurements.

Simultaneous Measurement using Capacitance and Ultrasonic Methods

In the second set of tests the seal was run against a steel counter face at a range of loads and speeds, simultaneously measuring ultrasonically and using capacitance. Figure 4 shows the raw data on an arbitrary y-axis. During the test sequence the speed has been ramped up and down and two loads have been used.

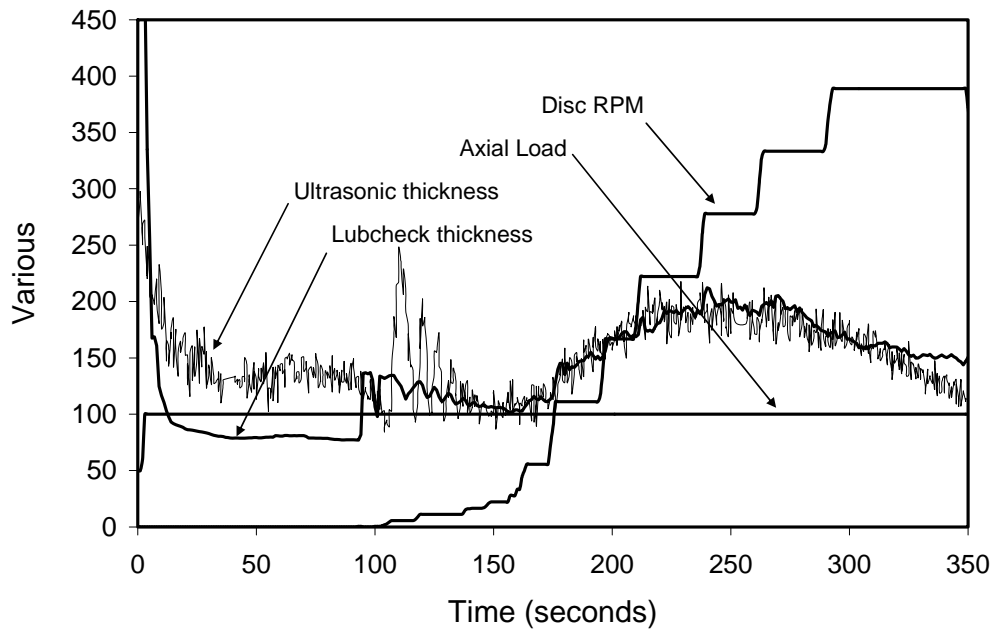


Figure 4. Plot of raw transducer output (on an arbitrary y-axis) for speed, load, capacitance and ultrasonically measured film thickness.

The ultrasonic measurement and the capacitance signal correlate closely. On figure 5 the two measurements are plotted against each other, for the whole test sequence. The correlation between the techniques is close to linear.

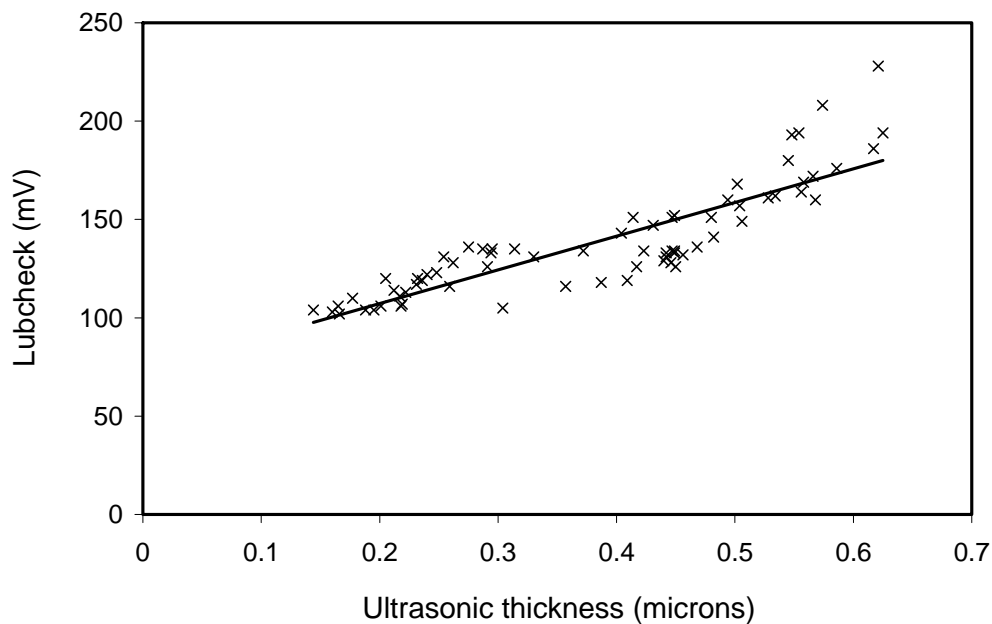


Figure 5. Plot of measured film capacitance against ultrasonically measured oil film thickness.

In figure 6 the ultrasonically measured film thickness is plotted against the rotational speed of the disk. Two curves are shown, one where the speed is increasing and one where it is decreasing. The points represent instantaneous measurements recorded at 0.5 s intervals. The solid lines are a ten point rolling average.

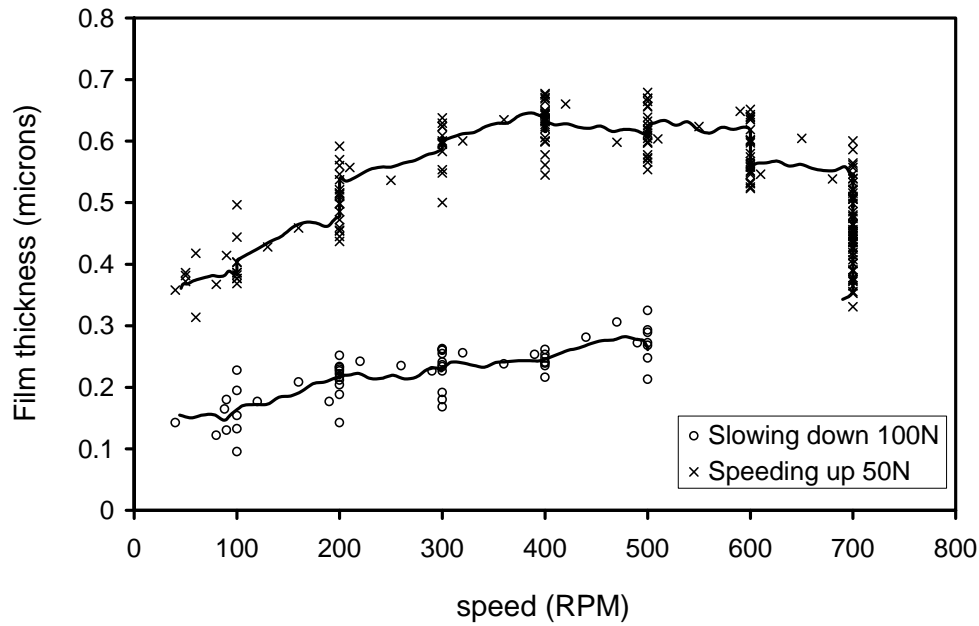


Figure 6. Plot of ultrasonically measured film thickness against disk rotational speed for two load cases.

Repeatability

The repeatability of measurements was studied by rotating a disc with a surface waviness against the instrument seal face and monitoring the oil film thickness continuously. This was a similar test to the one shown in figure 2, however the tests was run over a period of 1.5 hours, in which 40 rotations were recorded.

The resulting film thickness measurements for the 40 successive rotations of the seal were then median averaged, and compared with results, which exclude outliers, which fall in the 20% furthest from the median (possibly caused by air bubbles in the oil). The excellent conformity between the lines, shown in figure 7 shows the agreement between each measure of waviness and demonstrates the stability of the ultrasonic technique. The scatter is partly due to noise in the ultrasonic signal, but can also be attributed to the disk not following the same path with each rotation.

This result suggests that a median filter could be beneficial if the film thickness is measured on line as part of a seal condition monitoring system.

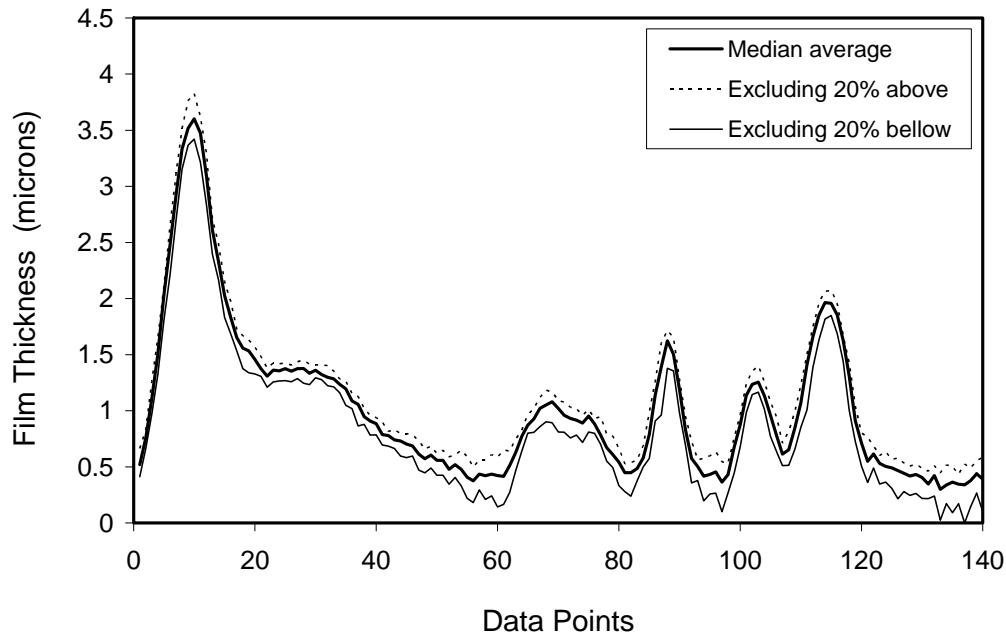


Figure 7. Plot showing median filtering of successive measures of waviness on the disk

3.3. Temperature Compensation

During the tests being run at high-speed, temperatures on the SiC ring ranged up to 140°C; this raises the several issues. The output from the ultrasonic transducers is affected by changes in temperature; amplitude decreases with increasing temperature. This is due to the temperature dependence of both the element itself and the properties of the adhesive layer between the element and the seal.

In addition, the speed of sound in oil, required for film thickness calculation is dependent on temperature. This relationship is approximately linear and is easily incorporated into the signal processing. The temperature dependence of the speed of sound in the T32 mineral oil used is 0.25%/degree.

These temperature effects are detrimental to the operation of the monitoring system, as an increase in temperature would signal an erroneous reduction on oil film thickness. In order to overcome this problem, the two separate approaches have been investigated as follows.

Curve fit Temperature Calibration

The temperature response of the sensing system was found by fastening a thermocouple to the element, and recording the output while heating the instrumented seal in a temperature controlled oven. The speed of sound in the oil was also measured (using a simple time of flight experiment) for a range of temperatures. Both responses were then used to compensate for temperature changes during testing.

Reference Pulse Temperature Calibration

To avoid the thermal calibration step an alternative self-compensating method was investigated. A second pulse was monitored, which was affected by temperature, but not dependant on the oil film. The effect of temperature on the transducer can then be isolated and removed from the measurement pulse. This method of temperature calibration is common practice for transducer calibration, see for example Shah et al [16].

There are several possibilities as to how this reference pulse is achieved, two examples are shown in figure 8, where pulses from the contact face and reference pulses are labelled c and r respectively. The first method devised was to attach a delay to the piezoelectric element in order to utilize the pulse reflected from the upper face of the specimen.

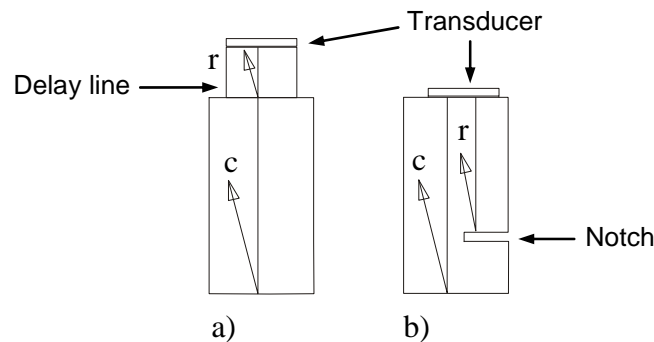


Figure 8. Diagram of the configuration used to obtain an extra reflection. a) Reference from delay line end. b) Reference from an intermediate notch

In order to test this approach, an ultrasonic transducer with a delay line was bonded to a face seal and the reflection from both the end of the delay line and the contact face of the seal were recorded (pulses r and c in figure 8). The resulting plots of amplitude vs. temperature are shown in figure 9 a).

Dividing the amplitude of each signal by their initial values shows by what fraction they decrease with temperature. The normalized plots obtained in this way are shown in figure 9 b). Both measurement and reference pulses reduce by the same proportion with respect to temperature; therefore the temperature variation for the delay line pulse may be used to compensate the oil film pulse.

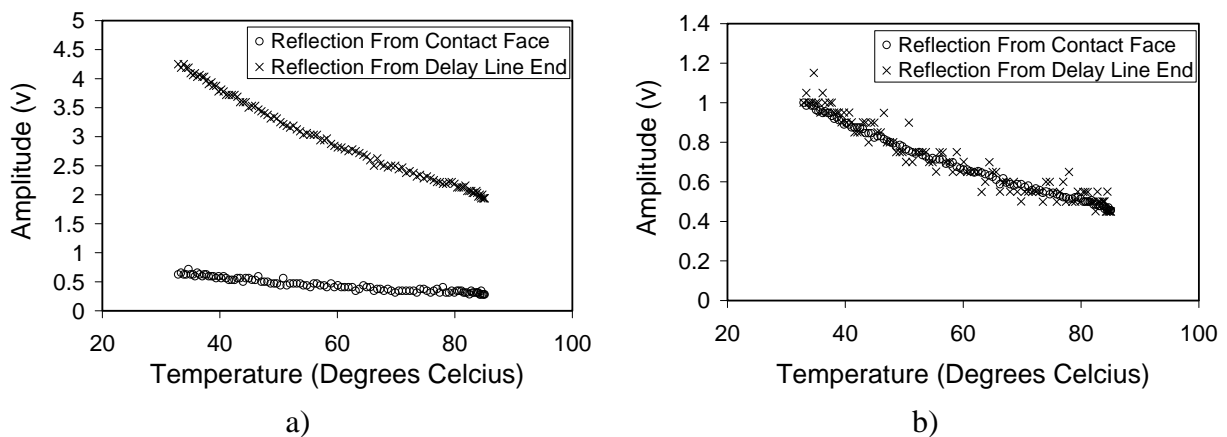


Figure 9. a) Plot of amplitude versus temperature for pulses from delay line end (r) and from contact face (c). b) Plot of normalized amplitude versus temperature for pulses from delay line end and from contact face.

A reference pulse can also be achieved by modification of the specimen geometry such that an extra pulse will be reflected. As shown in figure 8 b, this can be done by machining a step in the base of the specimen (if the design of the seal allows this) or by cutting a slot in the side of the specimen.

The disadvantage of this type of calibration is that it requires two ultrasonic signals both of which contribute noise to the resulting film thickness measurement. This increase in error is shown in figure 10, where film thickness is being measured in the seal. At time $t=100$ the notch calibration method has been introduced into the data processing. At this point the noise

in the signal noticeably increases. The standard deviation of the measured data was calculated, and was found to increase from 0.28 to 0.76 with the introduction of the notch calibration. In practice the decision whether to use this type of calibration will depend on the likelihood of temperature variation and the expected signal to noise ratio of the received signal.

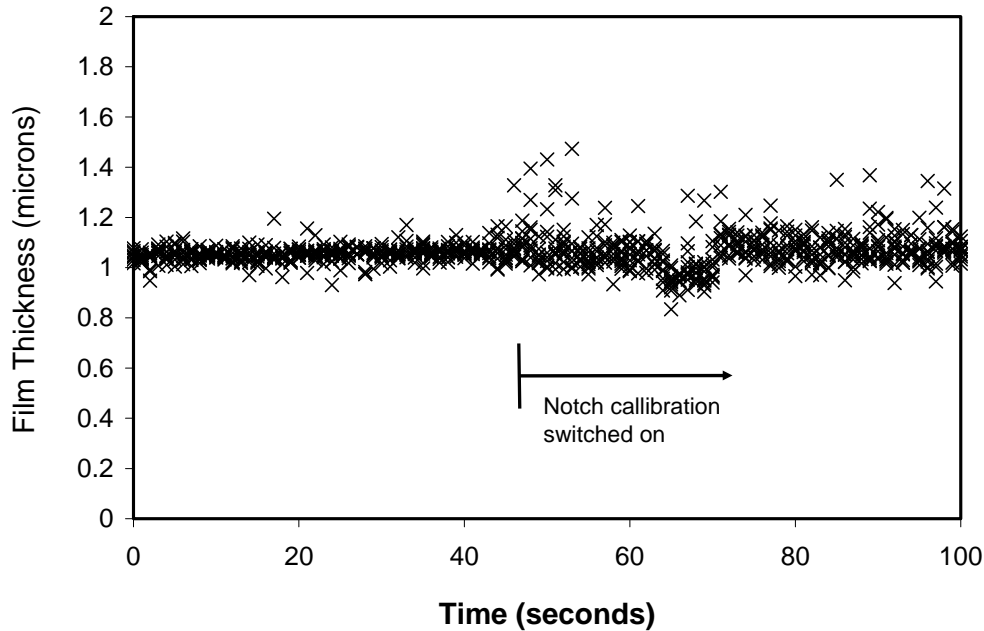


Figure 10. Film thickness vs. time, showing noisy effect of notch.

4. Experiments on a Seal Test Rig

4.1. Apparatus

The seal test rig shown schematically in figure 11 consisted of a shaft which was attached to the rotating face of the seal, housed inside a pressurized vessel. The shaft was driven by a variable speed electric motor. The loading of the seal faces was controlled by varying the pressure of the fluid surrounding the seal.

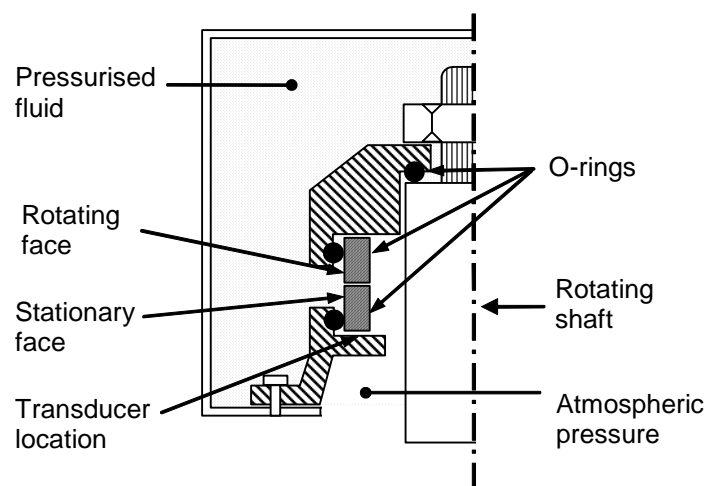


Figure 11. Schematic diagram of mechanical face seal

Three ultrasonic transducers were mounted on the seal ring equally spaced (120° apart), this redundancy was employed in case a wire snapped or a sensor failed. During the test programme all three sensors functioned adequately and gave very similar output.

The ultrasonic pulsing system and signal processing used were the same as that for the evaluation tests. References were taken for each sensor before the instrumented ring was assembled in the housing. Two variables influence the face seal operation, namely speed of rotation and pressure of the sealed fluid. In the following tests, speed and pressure are varied in different ways and the response of the fluid film inside the face seal is measured ultrasonically.

4.2. Results

Three Test Sensors

As a preliminary test, the apparatus was run and film thickness measured on each sensor for a short period in sequence. The results for this test are shown in figure 12, as expected the film thickness measured on each sensor is equal.

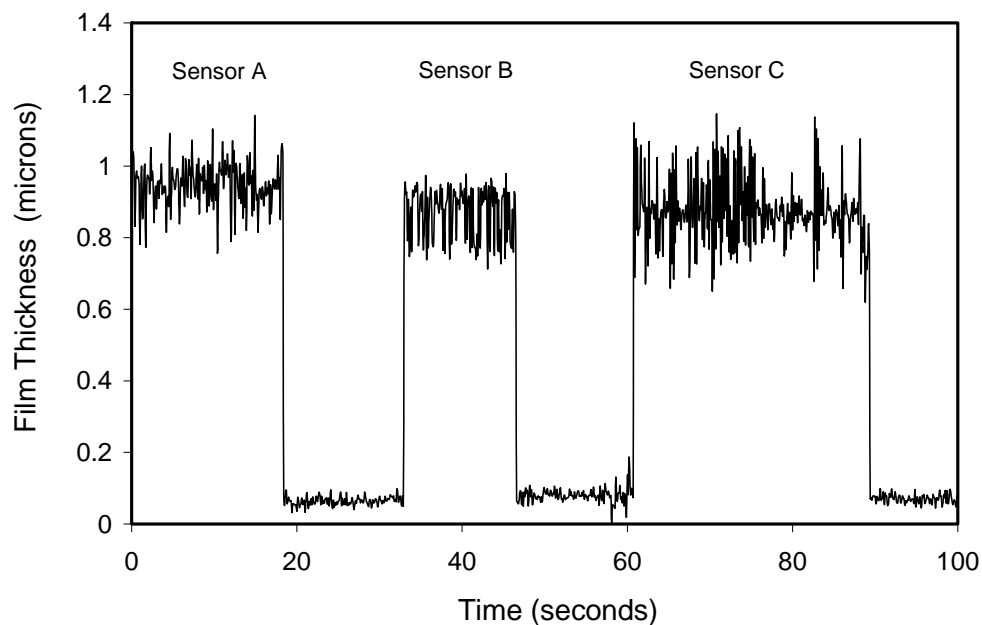


Figure 12. Oil film in seal measured on each sensor

Internal Pressure Variation

Film thickness was measured as the pressure was increased in steps while the shaft speed remained constant at 1000 rpm. This test was carried with both water and oil as the pressurized fluid. Figure 13 shows the response of the fluid film to the variation in pressure. The stability of the oil film is evident, while the water film is more sensitive to load; this is likely due to its lower viscosity. A large scatter in the results for the water film is evident; the cause of which is uncertain. Possibly this is due to some instability in the ultrasonic signal, however it is more likely due to the seal vibrating at the high speed with the water providing less damping than the viscous oil. Included in the figure is a plot of filtered film thickness, where only the local minima of film thickness values have been used.

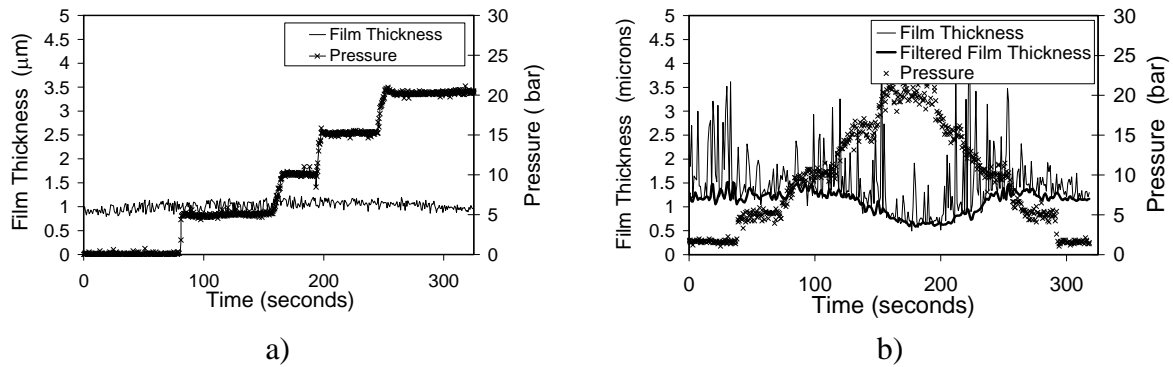


Figure 13. Plots of (a) oil film and (b) water film thickness variation with time as the sealed fluid pressure is varied. Constant shaft speed of 1000 rpm

Shaft Speed Variation

The following tests were devised in order to establish the response of the fluid film to changes in the rotational speed of the seal. Tests were carried out with both water and oil as the sealed fluid. The pressure was maintained at 10 bar while the speed of rotation of the seal was varied in steps. The response of the fluid films to variations in speed is displayed in figure 14. The fluid film is largely unaffected by the variation in speed. There is a large scatter in the results for the water film, similar to the pressure tests carried out with water; this suggests that the scatter is due to relative motion of the seal faces (vibration).

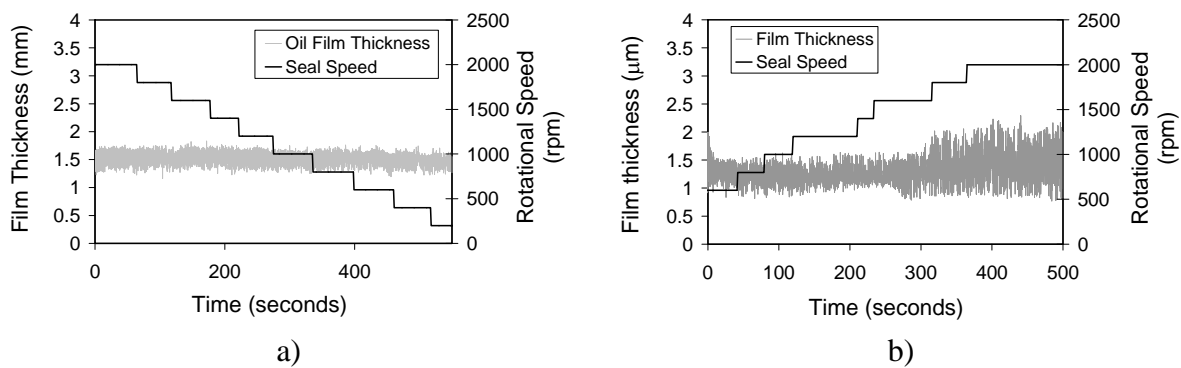


Figure 14. Plots of (a) oil film and (b) water film thickness variation with time as seal rotational speed is varied. Constant sealed fluid pressure of 10 bar.

Affects of Step Changes in Rotational Speed and Loading

The response of the seal to step changes in speed and pressure were studied. The results from this test are shown in figure 15, here the speed was reduced from 2000 rpm to 0 rpm in as short a time as the motor controller allowed, and then restarted to 2000 rpm. The oil film reduced dramatically as a result of these step changes as figure 15 shows, with film thickness reaching as low as 0.2µm. After three such stops, the seal was kept stationary, while the pressure was changed in rapid steps of 10 bar. This however had no significant effect on the oil film. The squeeze filmed formed after sudden shut down proved difficult to remove.

From figure 15 it can be seen that the noise in the measured film thickness is considerably less for the stationary seal, with the standard deviation of the measurements reducing from 0.131 to 0.095. This is likely due to the reduced vibration of the seal faces when stationary.

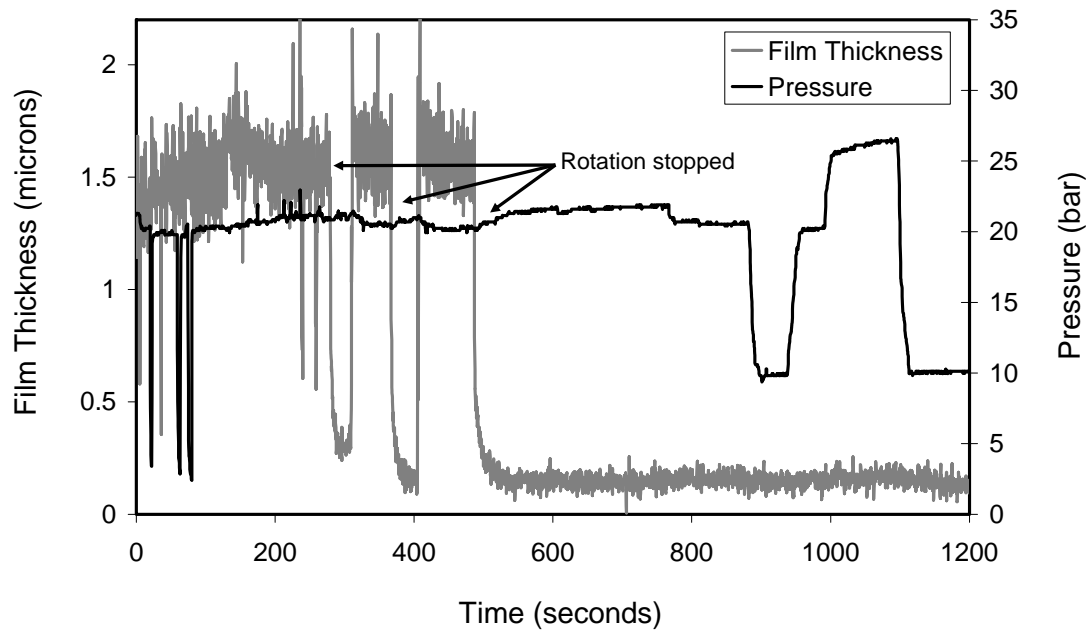


Figure 15. Plot of oil film thickness variation with time for a seal, subject to step changes in rotational speed and pressure (the recorded pressure signal is also shown).

It is important to note that the ultrasonic film thickness is measured successfully as rotation is rapidly stopped causing seal faces to come together. In an industrial application, before a seal fails, it is likely that, although less rapidly, the oil film will reduce in the same way. This therefore demonstrates that the effectiveness of the ultrasonic technique as a means of predicting failure in an industrial face seal condition monitoring application.

5. Discussion

The evaluation experiments show that ultrasonic reflection is an accurate method for measuring film thickness, with results being validated against established optical and capacitance techniques. The results obtained using the seal test rig demonstrates the ability of the technique to measure film thickness in an operating face seal. This indicates the potential of the technique as part of a condition monitoring system, used to predict seal failure and hence reduce leakage.

An advantage is that the approach is essentially non-invasive, requiring only that a low profile piezoelectric element to be glued to the back face of the stationary ring. There are limitations however regarding the seal materials. Firstly materials of high attenuation are a problem as they do not allow a reflected signal to be detected. This is however rarely an issue given most seal materials and geometries. The relative acoustic impedances of the two seal faces are a more important issue. Large acoustic impedance mismatch between seal faces reduces the range of possible reflection coefficient amplitude and therefore reduces the sensitivity of the measurement. Film thickness can be measured by this reflection amplitude method providing the acoustic impedances of the materials either side of the interface satisfy the approximate relationship $z_1/z_2 > 0.25$. Provided these conditions are satisfied then the technique can measure a wide range of oil films if the appropriate frequency transducer is used.

An important issue for practical implementation is the temperature sensitivity of the sensors. In most fluid sealing applications temperature is likely to fluctuate. This may need to be compensated for using the techniques described in this study. The approach is relatively simple but it does require either a pre-calibration of the sensor or slight modifications to the

seal design. Alternatively, there are other piezo-electric materials which are known to be less sensitive to temperature variation. Further work needs to be done to investigate these as an alternative basis for the sensor.

The presence of a second phase in the fluid film will upset the results. Small air bubbles will lead to a reduced effective speed of sound of the fluid mixture and hence an over prediction of the measured film thickness. Large air bubbles or voids will cause complete reflection of the signal. During these tests occasional air bubbles were observed (with the optical system) and these did indeed result in spikes in the recorded film thickness. Appropriate filtering and outlier extraction needs to be established for condition monitoring purposes.

Conclusions

An ultrasonic method of measuring a fluid film has been compared with optical interference and capacitance methods for a face seal application. The seal ring was assembled in a WAM5 rig where it could be tested against a glass disk (for optical measurements) and a steel disk (for electrical measurements).

The ultrasonic measurements were shown to vary linearly with capacitance as expected, over a range of loads and speeds. The film thickness ranges tested meant that a close comparison with an optical method could not be performed (because the two measuring ranges only coincided over a narrow film thickness region). However where the two methods overlapped a good agreement was observed.

Film thickness was successfully monitored as seal test rig as speed and load were varied. The results showed that, while stationary, the film thickness varied noticeably with load. When rotating however, the oil film remained relatively stable around 2 μm .

During normal operation of the seal, speed and load were stopped and started abruptly, in order to reproduce the condition of a seal failure. During these events, the measured film thickness was seen to drop dramatically down to 0.2 μm . This demonstrated the ability of the technique to predict failure in a face seal and therefore its aptitude for condition monitoring.

Acknowledgement

The authors are grateful to SKF ERC BV. and Huhnseal for access to experimental equipment and to Dr André van der Ham and Mr Jos Storcken of SKF and Mr Göran Anderberg of Huhnseal for their assistance, advice, and encouragement.

References

- [1] Lubbinge, H., (1999) On the lubrication of mechanical face seals, PhD thesis, University of Twente, The Netherlands.
- [2] Miettinen, J. and Siekkinen, V. (1995) Acoustic emission in monitoring sliding contact behaviour, *Wear*, Vol. 181-183, pp. 897-900.
- [3] Anderson, W. B., Jarzynski, J. and Salant, R. F., (2001), A condition monitor for liquid lubricated mechanical seals *Tribology Transactions*, Vol. 44, pp. 479-483.
- [4] Astridge, D.G. and Longfield, M.D., (1967), Capacitance Measurement and Oil Film Thickness in a Large Radius Disc and Ring Machine, *Proc. Instn. Mech, Engrs.*, Vol. 182, pp. 89-96.

- [5] Chu, P. S. Y., and Cameron, A. (1967), Flow of electric current through lubricated contacts, ASLE Transactions, Vol 10, pp.226-234.
- [6] El-Sisi, S.I. and Shawki, G.S.A., (1960), Measurement of Oil-Film Thickness Between Disks by Electrical Conductivity, Trans. ASME J. Basic Engng., Vol. 82D, pp.12-18.
- [7] Cameron, A. and Gohar, R., (1966), Theoretical and Experimental Studies of the Oil Film in Lubricated Point Contact, Proc. Roy. Soc. Lond., Vol. 291A, pp. 520-536.
- [8] Richardson, D.A. and Borman, G.L., (1991), Using Fibre Optics and Laser Fluorescence for Measuring Thin Oil Films with Applications to Engines, SAE Paper 912388.
- [9] Dwyer-Joyce, R.S., Drinkwater, B.W., and Donohoe, C.J., (2002), The Measurement of Lubricant Film Thickness using Ultrasound, Proc. Roy. Soc. Lond., Vol. 459, pp 957-976.
- [10] Dwyer-Joyce, R.S., Harper, P., and Drinkwater, B., (2004), 'A Method for the Measurement of Hydrodynamic Oil Films Using Ultrasonic Reflection', Tribology Letters, Vol. 17, pp. 337-348.
- [11] Dwyer-Joyce, R.S., Reddyhoff, T., and Drinkwater, B., (2004), 'Operating Limits for Acoustic Measurement of Rolling Bearing Oil Film Thickness', STLE Tribology Transactions, Vol. 47, pp. 366-375.
- [12] Kendall, K. and Tabor, D., (1971), An Ultrasonic Study of the Area of Contact between Stationary and Sliding Surfaces. Proc. R. Soc. Lond. Vol. 323, pp. 321-340.
- [13] Tattersall, H.G., (1973), the ultrasonic pulse-echo technique as applied to adhesion testing, J.Appl. Phys.D., Vol. 6, pp. 819-832.
- [14] Wikstrom, B. and Jacobson, B., (1997), Loss of lubricant from oil-lubricated near starved spherical roller bearings, IMechE part J, Vol. 211, J, pp 51-66.
- [15] Offterdinger, K. and Waschkies, E., (2003), Temperature dependence of the ultrasonic transmission through electrical resistance heating imperfect metal-metal interfaces, NDT&E International. Vol. 37, pp. 361-371.
- [16] Shah, V.V. and Balasubramaniam, K., (2000), Measuring Newtonian viscosity from the phase of reflected ultrasonic shear wave, Ultrasonics, Vol.38, pp. 921-927.
- [17] Reddyhoff, T., Kasolang, S., Dwyer-Joyce, and R.S., Drinkwater, B., (2005), The Phase Shift of an Ultrasonic Pulse at an Oil Layer and Determination of Film Thickness and Damping, IMechE part J, Vol. 219, pp.387-400.